Electrochemistry Communications 135 (2022) 107212

Contents lists available at ScienceDirect

Electrochemistry Communications

journal homepage: www.elsevier.com/locate/elecom

Recent progress in CO_2 reduction using bimetallic electrodes containing copper

Hannah L.A. Dickinson, Mark D. Symes *

WestCHEM, School of Chemistry, University of Glasgow, Glasgow G12 8QQ, United Kingdom

ARTICLE INFO

Keywords:
Carbon dioxide reduction
Electrocatalysis
Copper alloys
Copper bimetallics

ABSTRACT

Rising levels of carbon dioxide in the atmosphere have precipitated considerable research efforts aimed at generating energy from renewable sources, such that consuming this energy does not lead to further increases in atmospheric CO_2. Simultaneously, atmospheric CO_2 represents a useful feedstock for the storage of renewably-generated energy, in particular through electroreduction of CO_2 powered by renewables to give hydrocarbon fuels that when burned do not increase net CO_2 levels in the atmosphere. In order to bring such renewable-powered production of hydrocarbons from CO_2 to reality, improved electrocatalysts for carbon dioxide reduction are required. For example, Cu is the only single metal that demonstrates appreciable Faradaic efficiency for CO_2 reduction products that are reduced by more than two-electrons, but pure Cu is not an especially active or selective catalyst for this process. Hence there has been considerable interest in making bimetallic catalysts using Cu in combination with other metals in order to find systems that can reduce CO_2 to products such as methane, methanol, ethanol and beyond. In this minireview, we give an overview of recent progress in CO_2 electroreduction using bimetallic cathodes composed of copper and various other metals in combination, with a particular focus on studies going beyond two-electron reduction products from the last two years.

1. Introduction to CO_2 electroreduction

Climate change driven by the historically high levels of carbon dioxide in the atmosphere is one of the biggest challenges facing our society [1]. Electrochemical CO_2 reduction has been put forward as a viable technique to produce desirable hydrocarbon fuels (for example, as a means of storing renewably-generated power) which can be consumed without increasing the overall amount of CO_2 in the atmosphere, as part of a closed carbon cycle [2]. Electrochemical CO_2 reduction is a promising technique as it (1) often only requires ambient temperatures and pressures, (2) has the potential to be incorporated into existing renewable energy systems, and (3) the desired products can (in theory) be selected by changing parameters such as the applied potential and electrolyte [3]. A variety of products can be produced using electrochemical CO_2 reduction, some of which are listed in Table 1. The hydrogen evolution reaction (HER) is also shown, since this process is in constant competition with CO_2 reduction when protons are available.

The large number of products and possible reaction pathways (Fig. 1) means that selectivity for a given CO_2 reduction product can be poor and the energy efficiency for a desired product low. Thus, a variety of electrocatalysts, copper-based and otherwise, have been studied including pure metals [5], metal oxides [6], metal–ligand complexes [7] and graphitic carbon nitrides [8]. The presence of catalytically-active d-electrons and/or vacant orbitals of transition metals can allow the absorption and desorption of CO_2 and its products; metals are often chosen based on their binding strength towards a given reaction intermediate. Cu electrodes have gained attention for CO_2 electroreduction since Hori's seminal papers [9–11] wherein it was found that Cu displayed a unique activity towards the production of hydrocarbons compared to other pure metal electrodes. CO_2 reduction proceeds via multiple, simultaneous pathways, where all the reaction intermediates relate to each other in an approximately linear fashion [12]. To be selective for a single product these scaling relations must be broken; methods for this include ligand stabilisation, tethering, mixed metal phases and alloying [13].

Alloying is used in heterogeneous catalysis to tune the chemical environment at various binding sites. For example, the addition of a metal with a high oxygen affinity would aim to stabilise the *CHO intermediate relative to *CO (where * indicates a species that is adsorbed to the surface). Metals are combined, whether as alloys or separate

* Corresponding author.
E-mail address: mark.symes@glasgow.ac.uk (M.D. Symes).

https://doi.org/10.1016/j.elecom.2022.107212

Available online 11 January 2022

Table 1
Standard electrochemical potentials for CO_2 and proton reduction at 25 °C and 1 atm. [4]

Reaction	E°/ V vs. RHE
$CO_2 + e^- \rightarrow CO_2^{\bullet -}$	–1.48
$CO_2 + 2H^+ + 2e^- \rightarrow CO + H_2O$	–0.10
$CO_2 + 2H^+ + 2e^- \rightarrow HCOOH$	–0.19
$CO_2 + 4H^+ + 4e^- \rightarrow HCHO + H_2O$	–0.06
$CO_2 + 6H^+ + 6e^- \rightarrow CH_3OH + H_2O$	+0.03
$CO_2 + 8H^+ + 8e^- \rightarrow CH_4 + 2H_2O$	+0.17
$2CO_2 + 12H^+ + 12e^- \rightarrow C_2H_5OH + 3H_2O$	+0.09
$2CO_2 + 12H^+ + 12e^- \rightarrow C_2H_4 + 4H_2O$	+0.08
$2CO_2 + 14H^+ + 14e^- \rightarrow C_2H_6 + 4H_2O$	+0.14
$2H^+ + 2e^- \rightarrow H_2$	0.00

phases, to favour more complex and useful products than CO and H_2. The most effective catalysts will be highly selective towards a single multi-carbon product at a low overpotential. They will also be stable over long periods of time and multiple catalytic cycles.

In 1991, Watanabe published an investigation into Cu–M alloys where M = Ag, Cd, Ni, Pb, Sn and Zn; this was the first reported study into alloys for electrochemical CO_2 reduction [14]. The most noteworthy alloy was that of copper and nickel (Cu/Ni 90:10), which supressed CO production in favour of methanol at a peak Faradaic efficiency of 7% at –0.9 V vs. SHE. These results indicated a synergistic effect between Cu and Ni. This deviation from linear scaling relations has since been recognised as a combination of two effects: the electronic effect, which modifies the binding environment for intermediates, and the geometric effect, which changes the arrangement of the atoms at the active site [15].

A large variety of bimetallic materials have been investigated for CO_2 reduction, yet since Cu metal is unique in its ability to produce hydrocarbons, there is a particular focus on research into Cu–M bimetallics. Generally, the selectivity of Cu–M alloys is modified by varying the nature of M. Although this is simple in theory, results can be mixed, especially since the catalyst composition and metal arrangement both affect which reaction pathway dominates. This complexity continues to fascinate and tantalise many researchers. The use of copper and copper-based bimetallic catalysts for carbon dioxide electroreduction was reviewed by Su, Hwang and co-workers in 2018 [16], by Zhao et al at the start of 2020 [4], and by Xiao and Zhang [17] and Fontecave and co-workers [18] specifically for CO_2 reduction to C_2 products. However, considerable progress in the field continues to be made. In this review, we review some papers in this area that have emerged in the last two years. Even focussing on such recent works, it is impossible to be comprehensive in a minireview of this length. Hence we have chosen to focus our in-depth discussions on reports where carbon-based products that are more deeply reduced than two-electrons are obtained in significant Faradaic yield. A selection of pertinent Cu-based bimetallics published recently can be found in Table 2.

2. CO_2 electroreduction with bimetallic electrodes containing Cu

In recent years, several Cu-Ag based mixed metal catalysts with high selectivity towards methane have been developed. Choi et al.[21] synthesised Cu-Ag interfaces on the surface of Cu nanowires. Silver was chosen as Cu and Ag are essentially immiscible, thus the catalyst would contain a mixture of Ag and Cu phases rather than an alloy phase. It was suggested that the creation and maximisation of these atomic Ag-Cu interfaces would benefit electrochemical CO_2 reduction towards products beyond CO. After synthesis of the nanowires by galvanic displacement (Fig. 2), X-ray diffraction (XRD) confirmed that no alloyed CuAg phase was present and Energy Dispersive X-ray (EDX) mapping depicted a thin layer of Ag on the surface of the Cu nanowire. CO_2 reduction in a sealed H-cell revealed that the Cu_9Ag_1 catalyst displayed a Faradaic efficiency towards C_2H_4 of less than 21% across all potentials; however, the selectivity towards CH_4 was increased compared to pure Ag nanoparticles, which produced mainly CO, and pure Cu nanowires, whose highest reported Faradaic efficiencies were 55% ± 8% for CH_4 at −1.23 V_{RHE}, and 60% ± 4% for C_2H_4 at −1.06 V_{RHE}. Cu_9Ag_1 gave a maximum Faradaic efficiency for methane production of 72% at −1.17 V_{RHE}, decreasing to 66% ± 4% at –1.20 V_{RHE}. These are very high selectivities and Faradaic yields for methane; the challenge now will be to increase the relevant current densities (currently > 5 mA/cm^2) towards industrially relevant figures.

It is generally regarded that the reaction pathways towards CH_4 and C_2H_4 deviate after the formation of the *COH intermediate [39]: the addition of adsorbed hydrogen to this intermediate leads to CH_4 whilst coupling with CO leads the pathway towards C_2H_4, Fig. 3. Preferential CO binding on Ag is confirmed by electrochemical CO_2 reduction on Ag nanoparticles (Faradaic efficiency for CO > 90% at all potentials). In contrast, Cu promotes high hydrogen coverage at voltages more

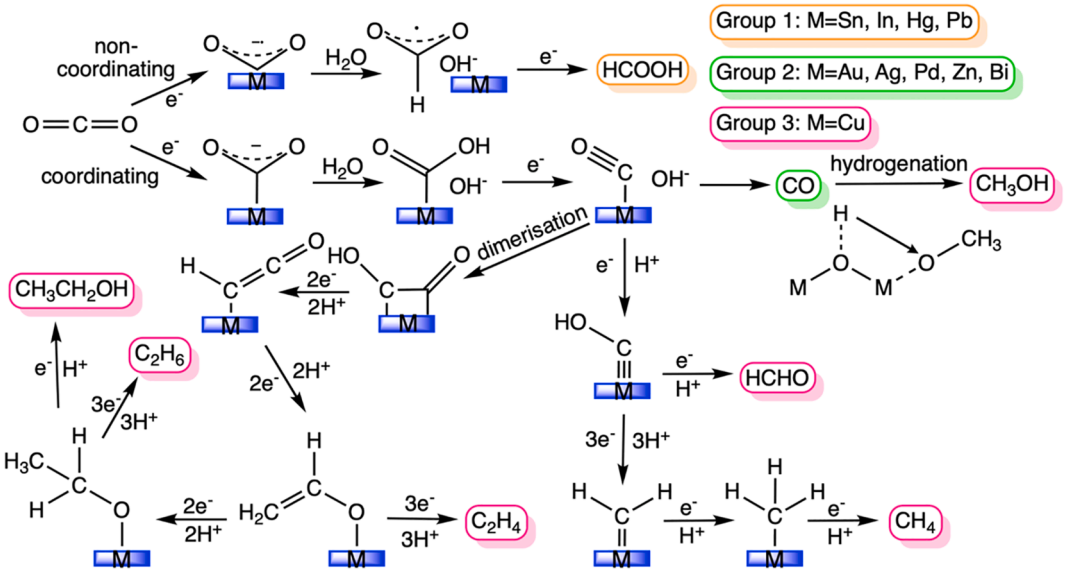

Fig. 1. Schematic of some of the possible CO_2 reduction pathways available on metal electrodes.

Table 2
Summary of recently reported Cu-based catalysts for electrochemical CO_2 reduction.

Electrode	Synthesis Technique	Morphology	Electrolyte	Potential (V vs. RHE)	Carbon product(s)	Faradaic Efficiency (%)	Ref
Cu-Ag	Physical vapour deposition	Pyramid textured	0.2 M $KHCO_3$	–1.1	Methane	62	Liu 2021 [19]
$Cu_{2.5}$-Ag_1 (Cu_1-Ag_1)	Electrophoretic deposition of nanoparticles	Spherical nanoparticles	0.1 M $KHCO_3$	–0.8	Methane (C_{2+} products)	20.6 (15.7)	Wu 2021 [20]
Cu_9Ag_1	Galvanic replacement of Cu nanowires	Nanowires	0.1 M $KHCO_3$	–1.17	Methane	72	Choi 2021 [21]
$Cu(Ag\text{-}20)_{20}$	Dropcasted Cu_2O nanowires and Ag powder	Composite Cu nanowire and Ag powder	0.1 M $KHCO_3$	–1.1	Ethanol	16.5	Ting 2020 [22]
3Au:1Cu	Modified Brust method	Nanoparticles	0.1 M $NaHCO_3$	–0.7	Formate	16	Shang 2021 [23]
$AuCu_3$@Au	Oxidative etching of $Au_{20}Cu_{80}$	3D bicontinuous nanoporous structure	0.1 M $KHCO_3$	–0.6	CO	97.27	Ma 2020 [24]
$CuAu_3$	Electrodeposition	Nanowire array	0.1 M $KHCO_3$	–0.5	Ethanol	48	Zhu 2019 [25]
Bi-Cu	Co-electrodeposition	Tight moss-like microstructure	0.5 M KOH / 0.5 M $KHCO_3$	–0.91	Formate	94.37	Peng 2021 [26]
Cu-Bi	Electrodeposition	Dendritic	0.5 M $KHCO_3$	–1.0	Formate	94.7 ± 2.8	Xiong 2021 [27]
Cu-Co (14% Co)	Electrodeposition	Small grain aggregates	0.1 M $KHCO_3$	–1.19	Methane	47.7	Takatsuji 2019 [28]
Cu-In	Electrodeposition	Dendritic	0.1 M $KHCO_3$	–0.85	Formate	87.4	Shao 2020 [29]
Cu-In/C	Co-reduction	Nanoparticles	0.1 M $KHCO_3$	–0.7	Syngas: ratios vary based on phase/ structure	H_2 = 39.8 CO = 24.3	Shen 2021 [30]
Ni-Cu (0.82% Ni)	Galvanic replacement of Cu nanowires	Nanowires	0.1 M KOH	–0.88	C_{2+} products	62	Zhang 2021 [31]
Cu-Ni (19 at% Ni)	Oxide-derived	Nanoparticles	0.05 M $KHCO_3$	–1.2	C_2 products	35	Suzuki 2020 [32]
Cu-Pd(1 0 0)	Thermal reduction treatment followed by in situ growth	Nanoparticles	0.1 M $KHCO_3$	–1.4	C_2 products	50.3 ± 1.2	Zhu 2021 [33]
Pd-Cu (70% Pd, 30% Cu)	Low-temperature solution method	Nanodendrites	0.1 M $KHCO_3$	–0.3	Formate	99.4	Zhou 2021 [34]
Sn-Cu	Lithography, electroplating of Cu film, and electroless coating of Sn nanoparticles	Cones	0.1 M $KHCO_3$	–0.6	CO	82.7	Dong 2021 [35]
$Cu_{6.26}Sn_5$	Electrochemical deposition	Dendritic rice spike-like	0.1 M $KHCO_3$	–1.08	Formate	97.8 ± 2.4	Li 2021 [36]
$CuZn_{20}$	Co-precipitation	Nanoparticles	0.1 M $KHCO_3$	–0.8	Ethanol (C_{2+} products)	34.25 (50.14)	Dongare 2021 [37]
MCu M = Cd (Sb, Pb, Zn)	Galvanic replacement reaction on sub-micron diameter copper rods	Nanofibers	0.5 M $NaHCO_3$	–1.05	Formate	70.5 (48.9, 58.7, 48.6)	Mosali 2019 [38]

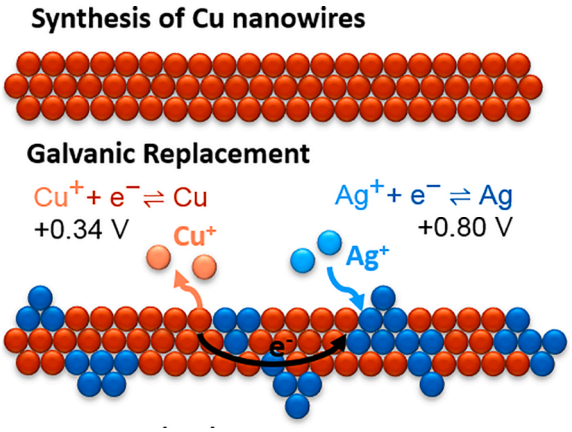

Fig. 2. Schematic of the preparation of Cu-Ag nanowires by galvanic replacement.

negative than –0.8 V_{RHE}. Thus, a synergistic effect based on *CO at Ag sites and *H on Cu could lead to higher selectivity towards CH_4 production.

Wu et al. exploited the immiscibility of Cu and Ag to develop mixed metal nanoparticles that were resistant to low-temperature catalyst sintering during electrochemical reduction [20]. As shown in Fig. 4, nanostructured Cu electrocatalysts have poor stability and a decreased active surface area caused by a degradation phenomenon that is widely ascribed to the agglomeration or dissolution-redeposition of smaller nanoparticles into larger ones [41].

Mixed Cu-Ag nanoparticles were prepared using an electrophoretic deposition method. Following electroreduction at –0.8 V_{RHE} notable sintering was seen by Scanning Electron Microscope (SEM) imaging on the pure Cu nanoparticles, whereas upon the addition of Ag nanoparticles, sintering was significantly reduced (Fig. 5). It was proposed that the immiscibility of the neighbouring Cu and Ag nanoparticles prevented dissolution and redeposition.

Although sintering was reduced, electrochemical CO_2 reduction on $Cu_{2.5}$-Ag_1 predominantly produced hydrogen. Initially, the highest Faradaic yield for a carbon-based product was 10.3% at −0.8 V_{RHE} towards methane. However, after the synthesis of a series of more dense Cu-Ag catalysts, to further investigate the stabilisation caused by Ag, it was found that the selectivity of the nanoparticle electrodes could be easily adapted by shifting the Cu:Ag ratio. Dense $Cu_{2.5}$-Ag_1 favoured methane production (FE_{CH4} 20.6% at −0.8 V_{RHE}), whilst a Cu:Ag ratio of 1:1 produced an enhanced activity towards C_{2+} products (Faradaic efficiency of 15.7% at −0.8 V_{RHE}), and Cu_1-$Ag_{2.5}$ was the best ratio for CO production. Although these efficiencies are not the highest seen in recent years, the increased catalyst stability, due to being sinter-resistant, could

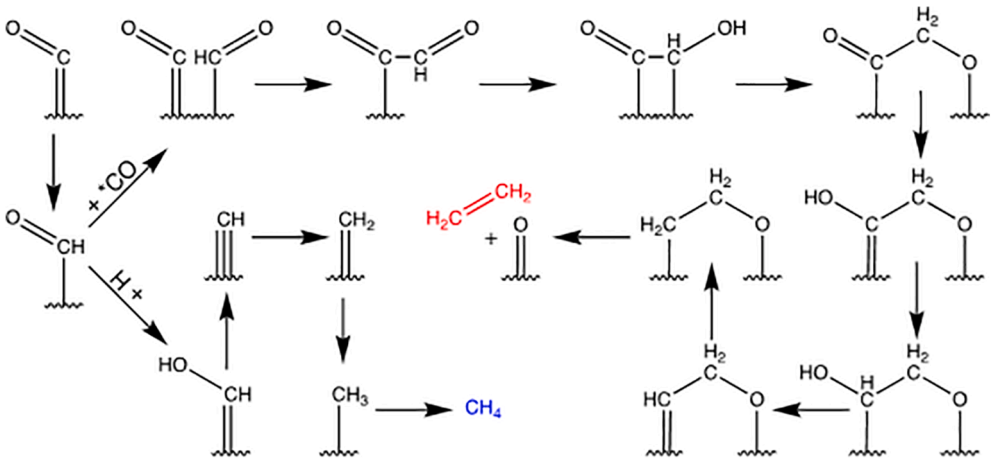

Fig. 3. Schematic of the possible reaction pathways towards methane [39] and ethylene [40].

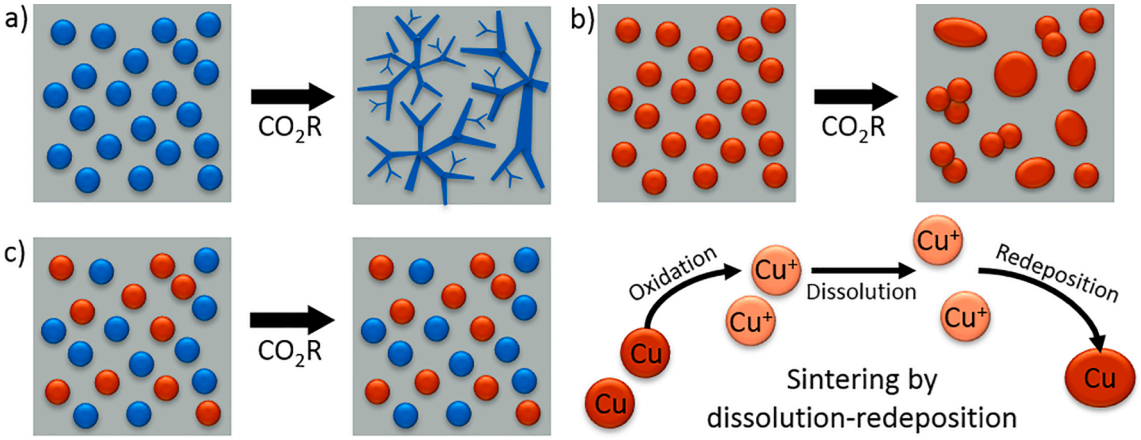

Fig. 4. Schematic showing the structural changes that occur to a) Ag, b) Cu, and c) Ag-Cu nanoparticles under CO_2 reduction ("CO_2R") conditions.

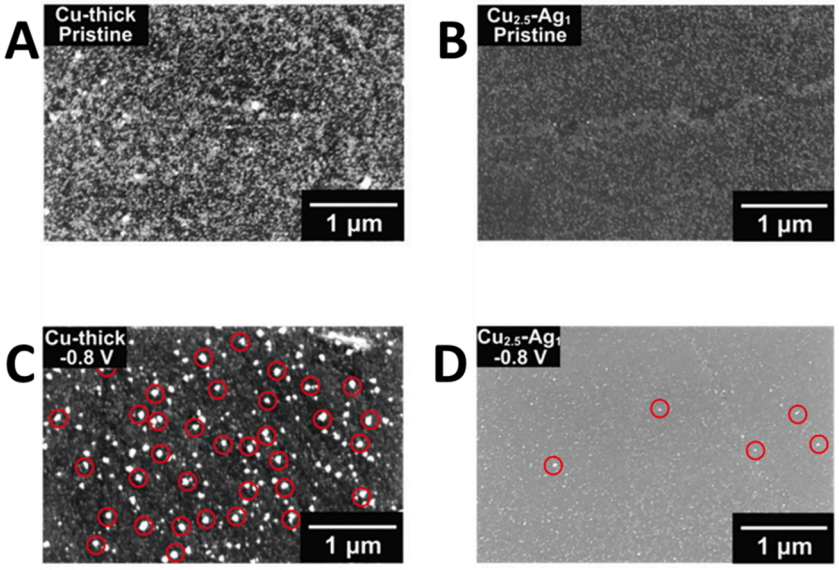

Fig. 5. SEM images of pure Cu nanoparticles ("Cu-thick") and a 2.5:1 Cu-Ag alloy ("$Cu_{2.5}$-Ag_1") before (panels A and B) and after (panels C and D respectively) performing the CO_2 reduction reaction at −0.8 V vs. RHE for 1 h. The red circles highlight nanoparticles that have sintered during the CO_2 reduction reaction. Adapted from reference [20]. (For interpretation of the references to colour in this figure legend, the reader is referred to the web version of this article.)

prove vital for applications.

Ting et al.[22] achieved increased CO_2 reduction activity towards ethanol via a composite catalyst containing oxide-derived Cu nanowires and Ag particles. It was found that ethanol production increased with the amount of CO evolved from Ag sites. Thus, in excess *CO, Ag and Cu worked in tandem to access a reaction pathway towards ethanol at a Faradaic efficiency of 16.5 % at −1.1 V_{RHE}. This pathway utilised the coupling of *CO + $*CH_x$ (x = 1, 2) at Cu-Ag boundaries which could then be reduced to ethanol.

Oxide-derived Cu-Ni alloy nanoparticles were developed by Suzuki et al.[32] with an enhanced selectivity towards ethylene and ethanol. Typically, Ni is regarded as increasing activity towards hydrogen evolution, binding *CO too strongly and effectively poisoning the catalyst surface.[42] Furthermore, theoretical calculations have suggested that no advantage will be seen upon alloying Ni with Cu compared to the activity of pure Cu [43]. However, it may be beneficial for an intermetallic catalyst to contain separated Ni as surface-bound or adjacent catalytic sites (which we note would agree with the results reported by Zhang et al [31] – see below). Ni could aid the production of C_{2+} products by providing the required *H.

After the initial synthesis of the Cu-Ni nanoparticles it was found that a pre-electrolysis activation step was required for more desirable (non-CO and H_2) products to be favoured. Cu-Ni (19 at% Ni) was found to show the best increase in the activity towards C_2 products, with a Faradaic yield for these species of 35%. Subsequently, H_2 evolution was greatly decreased to a Faradaic efficiency of 9%, compared to > 80% at 83 at% Ni, the highest nickel content tested. Given the dramatic change in activity, the surface of the catalyst was examined by X-ray Photoelectron Spectroscopy (XPS), which found that a mixture of Cu, Ni, Cu–O and Ni-O phases were present. Suzuki et al. maintain that the mixture of these components could be intrinsic to the amplified activity.

Previous density functional theory (DFT) calculations [39] indicated that CO_2 activation and CO dimerisation benefit from the electrostatic tension between Cu^0 and Cu^+; thus, it must be determined whether the presence of Ni is truly affecting the selectivity of the catalyst. It is possible that the electronic structures of the Cu active sites are altered by the adjacent Ni and Ni-O phases. Alternatively, Ni could supress a different pathway that does not lead to C_2 products, such as that towards HCOOH. There is also the possibility that an optimal dispersion of atomically disperse Ni sites on Cu could increase CO coverage enough to enhance the kinetics of C–C coupling without poisoning the surface [44]. Certainly, more exploration into the benefits of adjacent Ni sites on Cu is required.

Ni suffers from segregation within Cu-Ni alloys creating a non-uniform catalyst, thus Zhang et al.[31] developed a synthesis to deliberately create a highly dispersed Cu-Ni surface. Following their synthesis, Cu nanowires containing unsaturated sites were immersed in acetonitrile and $Ni(NO_3)_2$ for various time periods, 0.5–5 mins. The introduction of nitrile ligands from acetonitrile lowered the reduction potential of Cu, allowing galvanic replacement by Ni to occur.

CO_2 reduction was tested in a two-compartment H-cell using a CO_2-saturated 0.05 M $NaHCO_3$ solution as the electrolyte. CuNi (0.82 at% Ni) produced the most significant results, displaying a Faradaic yield for hydrogen of only 17% at −0.87 V_{RHE} and a Faradaic efficiency of 16% for ethanol production at −0.77 V_{RHE}, whilst the highest efficiency for C_2H_4 was recorded as 24% at −0.97 V_{RHE}. A volcano type relationship was observed when the amount of dispersed Ni was varied; a CuNi electrode with 0.13 at% Ni displayed only slightly higher activity towards C_2 products than pure Cu nanowires, and a CuNi mixture with 1.3 at% Ni mainly produced H_2 (with Faradaic yield ≥ 81% at all potentials). Thus, the increased activity towards C_2 products was ascribed to the intrinsic catalytic properties facilitated by the presence of both Cu and Ni at specific ratios. Further catalytic testing, in a flow-cell electrolyser in KOH electrolyte, allowed the activity of CuNi (0.82 at% Ni) to be optimised, with a measured Faradaic efficiency towards C_{2+} products of 62% at −0.88 V_{RHE}; similar increases in activity when using KOH in flow-cells have been reported before [45]. Whilst this CO_2 reduction activity is significant, further work is required to tune the selectivity towards specific C_2 products. DFT calculations were completed to learn more about the reaction pathways available on the CuNi catalyst. It was found that Ni decoration reduced the energy barrier for $*CO_2$, *COOH and *CO. The chemisorption of CO_2 was found to be the rate determining step. This work is significant in that it suggests that a bulk Cu-Ni alloy is not required in order to provide high activity for CO_2 reduction to C_{2+} products, but instead that decoration of only the surface is sufficient to endow the ability to perform such deep reductions.

ZnO is cheaper than most of the secondary metals that are normally combined with Cu for CO_2 electroreduction. Pure Zn gives low HER activity, mainly producing CO, so it is expected that the combination of Cu and Zn will further reduce levels of hydrogen evolution. The use of carbon-based materials as catalyst supports has also proven beneficial, with N-doped carbon in particular aiding CO_2 adsorption and activation.

CuO and ZnO-derived nanoparticles on N-doped graphene ($CuZn_x$/NGN) were synthesised using co-precipitation by Dongare et al. [37]. Those with a Zn loading of less than 20 wt% were evenly dispersed on the N-doped graphene; further Zn content led to agglomeration. Brunauer-Emmett-Teller (BET) analysis found the catalyst had a mesoporous structure which led to plentiful exposed active sites and high catalytic activity. Only liquid-phase product analysis was completed upon catalytic testing; the study focussed on the production of ethanol. On all catalysts, productivity towards ethanol increased with more negative potentials; $CuZn_{20}$/NGN showed the highest Faradaic yield for ethanol (34%) at –0.8 V_{RHE}.

Dongare et al. suggested a mechanism for the production of ethanol on $CuZn_{20}$/NGN wherein CO is generated on Zn and passed on to neighbouring CuO sites for further reduction towards ethanol. It has been proposed that C–C coupling between hydrogenated C_1 species is more favourable than the combination of two *CO species [46]. Thus, a mechanism containing the coupling of $*CH_2$ with *CO was proposed (Fig. 6). According to this mechanism, CO_2 is absorbed on Cu, Zn, and pyridinic-N sites, where proton-electron transfers occur to produce *CO. Then hydrogenation forms $*CH_2$ which can couple to the *COH generated at neighbouring sites to give $*CH_2COH$. A final hydrogenation step and release from the catalysis surface gives ethanol. However, this suggested mechanism does not reveal how each individual site, or the mixture of Cu and Zn sites is beneficial. Computational analysis based on this mechanism could be useful in this regard.

3. Conclusions and outlook

In this minireview, we have given a short overview of some of the more recent developments in the field of the CO_2 electroreduction with bimetallic copper cathodes. The main focus of our overview was on systems that are capable of reducing CO_2 by more than two electrons (producing species of more interest and utility than CO and formic acid/formate). Cu-based Ni and Zn catalysts are currently the most promising in this regard, with C_{2+} products having been successfully reported at significant Faradaic efficiencies. However, it is perhaps somewhat surprising how few are the reports of deeper reduction of CO_2 beyond two electrons compared to the reports for CO and/or formate production. This is probably the biggest challenge facing the field at the current time. Electrochemical reduction of CO_2 to CO can be performed in aqueous solution at current densities in excess of 0.8 A cm^{-2} with Faradaic yields > 98% [47]. In many respects then, electrochemical reduction of CO_2 by two electrons is a solved problem. The challenge for the community now is to devise ways in which CO_2 may be cleanly and efficiently reduced by more than two electrons, so as to access species with multiple carbon–carbon bonds, and so to produce genuine chain hydrocarbons. The reports that we have highlighted in this minireview point the way towards this goal, but clearly significant knowledge gaps remain. A deep mechanistic understanding behind why particular bimetallic combinations are effective (whilst others are less so) is required. The field would

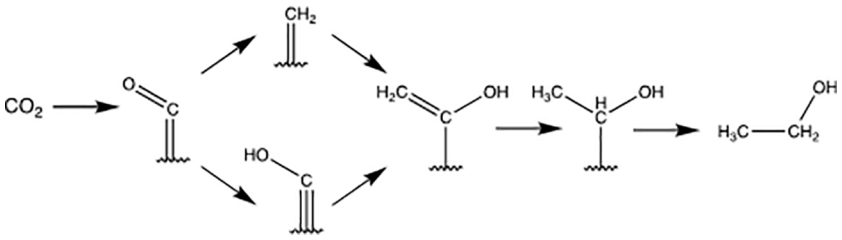

Fig. 6. Schematic of the possible reaction pathways towards ethanol outlined by Dongare et al.

also benefit from a more systematic approach in terms of how materials are screened and selected [48]; this can only aid in the discovery of catalysts capable of reducing CO_2 by more than two electrons. Finally, a wider selection of materials needs to be screened in depth, including (but not limited to) molecular systems and more complex multi-metallic catalysts. By careful and systematic study, leveraging some of the recent progress in the field as summarised above, the dream of selectively electro-reducing CO_2 to multi-carbon products can be made a reality.

CRediT authorship contribution statement

Hannah L.A. Dickinson: Writing – original draft. **Mark D. Symes:** Writing – review & editing.

Declaration of Competing Interest

The authors declare that they have no known competing financial interests or personal relationships that could have appeared to influence the work reported in this paper.

Acknowledgments

The authors thank the EPSRC for funding (EP/R020914/1) and MDS thanks the Royal Society for a University Research Fellowship (UF150104).

References

[1] K. Prashant, Front. Sustain. Cities 3 (2021), 645613.
[2] P. De Luna, C. Hahn, D. Higgins, S.A. Jaffer, T.F. Jaramillo, E.H. Sargent, Science 364 (2019) eaav3506.
[3] Z. Sun, T. Ma, H. Tao, Q. Fan, B. Han, Chem 3 (2017) 560–587.
[4] J. Zhao, S. Xue, J. Barber, Y. Zhou, J. Meng, X. Ke, J. Mater. Chem. A 8 (2020) 4700–4734.
[5] J. Qiao, Y. Liu, F. Hong, J. Zhang, Chem. Soc. Rev. 43 (2014) 631–675.
[6] E. Tayyebi, J. Hussain, Y. Abghoui, E. Skúlason, J. Phys. Chem. C 112 (2018) 10078–10087.
[7] R. Francke, B. Schille, M. Roemelt, Chem. Rev. 118 (2018) 4631–4701.
[8] Q. Lu, K. Eid, W. Li, A.M. Abdullah, G. Xu, R.S. Varma, Green Chem. 23 (2021) 5394–5428.
[9] Y. Hori, A. Murata, R. Takahashi, J. Chem. Soc., Faraday Trans. 1 (85) (1989) 2309–2326.
[10] Y. Hori, H. Wakebe, T. Tsukamoto, O. Koga, Electrochim. Acta 39 (1994) 1833–1839.
[11] Y. Hori, K. Kikuchi, S. Suzuki, Chem. Lett. (1985) 1695–1698.
[12] A. Peterson, J.K. Nørskov, J. Phys. Chem. Lett. 3 (2012) 251–258.
[13] Y. Li, Q. Sun, Adv. Energy Mater. 6 (2016) 1600463.
[14] M. Watanabe, M. Shibata, A. Kato, M. Azuma, T. Sakata, J. Electrochem. Soc. 138 (1991) 3382–3389.
[15] J. He, N.J.J. Johnson, A. Huang, C.P. Berlinguette, ChemSusChem 11 (2018) 48–57.
[16] M.K. Birhanu, M.-C. Tsai, A.W. Kahsay, C.-T. Chen, T.S. Zeleke, K.B. Ibrahim, C.-J. Huang, W.-N. Su, B.-J. Hwang, Adv. Mater. Interfaces 5 (2018) 1800919.
[17] C. Xiao, J. Zhang, ACS Nano 15 (2021) 7975–8000.
[18] D. Karapinar, C.E. Creissen, J.G. Rivera de la Cruz, M.W. Schreiber, M. Fontecave, ACS Energy Lett. 6 (2021) 694–706.
[19] Y. Liu, H. Qiu, J. Li, L. Guo, J.W. Ager, A.C.S. Appl, Mater. Interfaces 13 (2021) 40513–40521.
[20] L. Wu, K.E. Kolmeijer, Y. Zhang, H. An, S. Arnouts, S. Bals, T. Altantzis, J. P. Hofmann, M. Costa Figueiredo, E.J.M. Hensen, B.M. Weckhuysen, W. van der Stam, Nanoscale 13 (2021) 4835–4844.
[21] C. Choi, J. Cai, C. Lee, H.M. Lee, M. Xu, Y. Huang, Nano Res. 14 (2021) 3497–3501.
[22] L.R.L. Ting, O. Piqué, S.Y. Lim, M. Tanhaei, F. Calle-Vallejo, B.S. Yeo, ACS Catal. 10 (2020) 4059–4069.
[23] H. Shang, D. Kim, S.K. Wallentine, M. Kim, D.M. Hofmann, R. Dasgupta, C. J. Murphy, A. Asthagiri, L.R. Baker, Chem. Sci. 12 (2021) 9146–9152.
[24] X. Ma, Y. Shen, S. Yao, C. An, W. Zhang, J. Zhu, R. Si, C. Guo, C. An, J. Mater. Chem. A 8 (2020) 3344–3350.
[25] W. Zhu, K. Zhao, S. Liu, M. Liu, F. Peng, P. An, B. Qin, H. Zhou, H. Li, Z. He, J. Energy Chem. 37 (2019) 176–182.
[26] L. Peng, Y. Wang, Y. Wang, N. Xu, W. Lou, P. Liu, D. Cai, H. Huang, J. Qiao, Appl. Catal. B 288 (2021), 120003.
[27] Y. Xiong, B. Wei, M. Wu, B. Hu, F. Zhu, J. Hao, W. Shi, J. CO2 Util. 51 (2021), 101621.
[28] Y. Takatsuji, I. Nakata, M. Morimoto, T. Sakakura, R. Yamasaki, T. Haruyama, Electrocatalysis 10 (2019) 29–34.
[29] J. Shao, Y. Wang, D. Gao, K. Ye, Q. Wang, G. Wang, Chinese, J. Catal. 41 (2020) 1393–1400.
[30] C. Shen, P. Wang, L. Li, X. Huang, Q. Shao, Nano Res. (2021), https://doi.org/10.1007/s12274-021-3512-y.
[31] X. Zhang, C. Liu, Y. Zhao, L. Li, Y. Chen, F. Raziq, L. Qiao, S.-X. Guo, C. Wang, G. G. Wallace, A.M. Bond, J. Zhang, Appl. Catal. B 291 (2021), 120030.
[32] T.M. Suzuki, T. Ishizaki, S. Kosaka, N. Takahashi, N. Isomura, J. Seki, Y. Matsuoka, K. Oh-Ishi, A. Oshima, K. Kitazumi, K. Sekizawa, T. Morikawa, Chem. Commun. 56 (2020) 15008–15011.
[33] L. Zhu, Y. Lin, K. Liu, E. Cortés, H. Li, J. Hu, A. Yamaguchi, X. Liu, M. Miyauchi, J. Fu, M. Liu, Chinese J. Catal. 42 (2021) 1500–1508.
[34] R. Zhou, X. Fan, X. Ke, J. Xu, X. Zhao, L. Jia, B. Pan, N. Han, L. Li, X. Liu, J. Luo, H. Lin, Y. Li, Nano Lett. 21 (2021) 4092–4098.
[35] W.J. Dong, J.W. Lim, J.Y. Park, C.J. Yoo, S. Baek, W.S. Cho, W. Kim, J.-L. Lee, Appl. Surf. Sci. 565 (2021), 150460.
[36] D. Li, L. Huang, Y. Tian, T. Liu, L. Zhen, Y. Feng, Appl. Catal. B 292 (2021), 120119.
[37] S. Dongare, N. Singh, H. Bhunia, Appl. Surf. Sci. 556 (2021), 149790.
[38] V.S.S. Mosali, X. Zhang, Y. Zhang, T. Gengenbach, S.-X. Guo, G. Puxty, M.D. Horne, A.M. Bond, J. Zhang, A.C.S. Sustain, Chem. Eng. 7 (2019) 19453–19462.
[39] T. Cheng, H. Xiao, W.A. Goddard, Proc. Natl. Acad. Sci. USA 114 (2017) 1795–1800.
[40] J. Garza, A.T. Bell, M. Head-Gordon, ACS Catal. 8 (2018) 1490–1499.
[41] E.D. Goodman, J.A. Schwalbe, M. Cargnello, ACS Catal. 7 (2017) 7156–7173.
[42] R. Kortlever, J. Shen, K.J.P. Schouten, F. Calle-Vallejo, M.T.M. Koper, J. Phys. Chem. Lett. 6 (2015) 4073–4082.
[43] P. Hirunsit, W. Soodsawang, J. Limtrakul, J. Phys. Chem. C 119 (2015) 8238–8249.
[44] H.B. Yang, S.-F. Hung, S. Liu, K. Yuan, S. Miao, L. Zhang, X. Huang, H.-Y. Wang, W. Cai, R. Chen, J. Gao, X. Yang, W. Chen, Y. Huang, H.M. Chen, C.M. Li, T. Zhang, B. Liu, Nat Energy 3 (2018) 140–147.
[45] C. Dinh, T. Burdyny, M.G. Kibria, A. Seifitokaldani, C.M. Gabardo, F.P. Garcia de Arquer, A. Kiani, J.P. Edwards, P. De Luna, O.S. Bushuyev, C. Zou, R. Quintero-Bermudez, Y. Pang, D. Sinton, E.H. Sargent, Science 360 (2018) 783–787.
[46] J.H. Montoya, A.A. Peterson, J.K. Nørskov, ChemCatChem 5 (2013) 737–742.
[47] S.S. Bhargava, F. Proietto, D. Azmoodeh, E.R. Cofell, D.A. Henckel, S. Verma, C. J. Brooks, A.A. Gewirth, P.J.A. Kenis, ChemElectroChem 7 (2020) 2001–2011.
[48] J. He, K.E. Dettelbach, D.A. Salvatore, T. Li, C.P. Berlinguette, Angew. Chem. Int. Ed. 56 (2017) 6068–6072.